available at www.sciencedirect.com

ScienceDirect

www.elsevier.com/locate/brainres

BRAIN RESEARCH

Research Report

Chronic 835-MHz radiofrequency exposure to mice hippocampus alters the distribution of calbindin and GFAP immunoreactivity

Dhiraj Maskey[a], *Jonu Pradhan*[b], *Bijay Aryal*[c], *Chang-Min Lee*[d], *In-Young Choi*[a], *Ki-Sup Park*[a], *Seok Bae Kim*[e], *Hyung Gun Kim*[c,*], *Myeung Ju Kim*[a,*]

[a]*Department of Anatomy, Dankook University College of Medicine, Cheonan, Chungnam, South Korea*
[b]*Department of Physiology, Dankook University College of Medicine, Cheonan, Chungnam, South Korea*
[c]*Department of Pharmacology, Dankook University College of Medicine, Cheonan, Chungnam, South Korea*
[d]*Department of Neurology, Dankook University College of Medicine, Cheonan, Chungnam, South Korea*
[e]*Department of Internal Medicine, Dankook University College of Medicine, Cheonan, Chungnam, South Korea*

ARTICLE INFO

Article history:
Accepted 11 May 2010
Available online 17 June 2010

Keywords:
Radiofrequency
Calcium
Calbindin
Glial fibrillary acidic protein (GFAP)
Hippocampus

ABSTRACT

Exponential interindividual handling in wireless communication system has raised possible doubts in the biological aspects of radiofrequency (RF) exposure on human brain owing to its close proximity to the mobile phone. In the nervous system, calcium (Ca^{2+}) plays a critical role in releasing neurotransmitters, generating action potential and membrane integrity. Alterations in intracellular Ca^{2+} concentration trigger aberrant synaptic action or cause neuronal apoptosis, which may exert an influence on the cellular pathology for learning and memory in the hippocampus. Calcium binding proteins like calbindin D28-K (CB) is responsible for the maintaining and controlling Ca^{2+} homeostasis. Therefore, in the present study, we investigated the effect of RF exposure on rat hippocampus at 835 MHz with low energy (specific absorption rate: SAR = 1.6 W/kg) for 3 months by using both CB and glial fibrillary acidic protein (GFAP) specific antibodies by immunohistochemical method. Decrease in CB immunoreactivity (IR) was noted in exposed (E1.6) group with loss of interneurons and pyramidal cells in CA1 area and loss of granule cells. Also, an overall increase in GFAP IR was observed in the hippocampus of E1.6. By TUNEL assay, apoptotic cells were detected in the CA1, CA3 areas and dentate gyrus of hippocampus, which reflects that chronic RF exposure may affect the cell viability. In addition, the increase of GFAP IR due to RF exposure could be well suited with the feature of reactive astrocytosis, which is an abnormal increase in the number of astrocytes due to the loss of nearby neurons. Chronic RF exposure to the rat brain suggested that the decrease of CB IR accompanying apoptosis and increase of GFAP IR might be morphological parameters in the hippocampus damages.

* *Corresponding authors*. Hyung Gun Kim is to be contacted at Department of Pharmacology, Dankook University, College of Medicine, San 29, Anseo-Dong, Cheonan, Chungnam, South Korea. Fax: +82 41 550 3866. Myeung Ju Kim, Department of Anatomy, Dankook University, College of Medicine, San 29, Anseo-Dong, Cheonan, Chungnam, South Korea. Fax: +82 41 550 3905.
E-mail addresses: hgkimm@dankook.ac.kr (H.G. Kim), mjukim99@dku.edu (M.J. Kim).

0006-8993/$ – see front matter © 2010 Elsevier B.V. All rights reserved.
doi:10.1016/j.brainres.2010.05.045

1. Introduction

Explosive growth of wireless mobile communication in the number of users and rapid worldwide expansion has been observed over the last three decades (Feychting et al., 2005). Mobile phones operate at frequencies between 400–900 MHz in analog system and 1.8–2.2 GHz in digital system (International Commission for Non-Ionizing Radiation Protection, 2004). Mobile phone users often suffered from headaches, heat sensation during long time communication (Frey, 1998; Hocking, 1998), including abnormal electroencephalogram (EEG) recording patterns and sleep stage disturbances (Wagner et al., 1998; Borbely et al., 1999). These observations have raised concerns about possible biological effects of radiofrequency (RF) electromagnetic field (EMF) exposure to the human body. The nervous system, especially the brain due to its close proximity to RF source, is exposed to relatively high specific absorption rate (SAR) compared to rest of the body (Mausset et al., 2001; Odaci et al., 2008). The potential effect of RF on the release of neurotransmitters, blood–brain barrier (BBB) permeability, and behavioral changes has been noted in various *in vivo* animal and human studies (Brillaud and de Seze, 2006; D'Andrea et al., 2003).

The possible effect of RF exposure on nervous system has prompted investigations with animal models mostly focusing on biochemical and morphological alterations. Neuronal damages to the cortex, hippocampus, cerebellum, and basal ganglia due to RF exposure have also been reported earlier (Mausset et al., 2001; Salford et al., 2003). The intimate relationship between EMF emitted by mobile phones and brain function has also been studied with regards to sleep disorder (Hamblin and Wood, 2002), attention deficits (Edelstyn and Oldershaw, 2002), neuronal survival, learning, and memory processing (Manikonda et al., 2007; Koivisto et al., 2000a,b; Preece et al., 1999). The biological effects of EMF in the cellular level are also reported in the alteration of intracellular signaling pathways through changes in ionic distribution and membrane fluidity (Hossmann and Hermann, 2003) or alteration in calcium (Ca^{2+}) ion permeability across cell membranes (Adey, 1981). Despite several biological, epidemiological, and toxicological studies, the potential adverse effects of EMF exposure on the central nervous system (CNS) are still controversial (Hietanen, 2006).

Ca^{2+} plays an important role in the neurotransmitter release and action potential generation as well as membrane integrity and function in the nervous system (Blackman, 1992). The effect of RF radiation on homeostatic Ca^{2+} function such as alteration of Ca^{2+} binding in the membrane, Na^+ K^+-ATPase activity (Behari et al., 1998), Ca^{2+}-ATPase activity, cell permeability, and central cholinergic activity (Kunjilwar and Behari, 1993), which can result in tumorigenesis and neural degeneration, were previously suggested. Ca^{2+} mobilization on nervous system has also been observed, that is, RF exposure induces Ca^{2+} efflux from brain tissues and isolated neurons of different species (Bawin et al., 1978; Adey et al., 1982; Dutta et al., 1984, 1989). The effect of RF EMF on the nervous system might be caused by the alteration in the cellular Ca^{2+} concentration.

The maintenance of Ca^{2+} concentration is attributable to the buffering effect of calcium binding proteins (CaBPs) consisting of several calcium binding motifs for binding Ca^{2+} with high affinity, which belong to the EF hand proteins though efflux, and influx of Ca^{2+} via various calcium channels is also required (Celio et al., 1996). CaBPs have been implicated as important regulators in the pathological process of neuronal degeneration (Airaksinen et al., 1997) because CaBP, by virtue of its ability to buffer Ca^{2+}, acts to protect neurons from Ca^{2+}-mediated toxic injury (Miller, 1995). A cytosolic CaBP, calbindin D28-k (CB), is involved in intracellular Ca^{2+} regulation with neuroprotective role due to its buffering capability (Mattson et al., 1991). It is used as a marker of neuronal population (Pfeiffer et al., 1989) and also implicated as an important regulator of neuronal degeneration (Liang et al., 1996). The neuronal loss and the morphological changes of glial cells are associated with the pathological changes (Miguel-Hidalgo et al., 2002).

Glial cells like astrocyte, comprising a large part of brain, play a role in neurotransmission and control of blood–CNS interface as well as in nourishment and protection to neurons (Eddleston and Mucke, 1993). Astrocytes are capable of regulating synaptic neurotransmission and neuronal activity (Araque et al., 2001) and respond to changes in the intracellular free Ca^{2+} concentration. Since glial fibrillary acidic protein (GFAP), an intermediate filament protein, is frequently used as a well-known marker for astrocyte (Eng, 1985; Norton et al., 1992; Eng et al., 2000), increased expression of glial fibrillary acidic protein (GFAP) has often been recognized in brain injury (Eng and Shiurba, 1988). In the same way, the disturbance of Ca^{2+} homeostasis has been also known to be linked with increase of GFAP immunoreactivity (IR) after brain injury (Lee et al., 2000).

Sequential molecular responses resulting from altered intracellular Ca^{2+} concentration in the brain may trigger the variation of synaptic strength, which contribute to the disturbance of synaptic activity (Lisman, 1989; Artola and Singer, 1993) such as the learning and memory mechanism in the hippocampus. Considering the critical role of CaBP Ca^{2+} homeostasis in numerous processes for cellular preservation, modulation of intracellular Ca^{2+} concentration by CB could play an important part in preserving hippocampus function. Therefore, we investigated the effect of RF on mice hippocampus at 835 MHz at specific absorption rate (SAR) 1.6 W/kg after 3 months of exposure to indicate brain damage by using both CB and GFAP specific antibodies as immunohistochemical method and TUNEL assay.

2. Results

2.1. *Histopathological observations*

2.1.1. *Calbindin Immunoreactivity*

The CB IR in the hippocampal formation of sham control (SC) group was mainly observed in soma and dendrites of the pyramidal cells and interneurons. A large number of stained cells in the stratum pyramidale were distinctly observed in the CA1 area of SC group (Figs. 1A and B). The cells present in the different layers of CA1 area displayed CB IR with varying intensity in the SC group. Single neurons displayed intense labeling in stratum oriens, stratum radiatum, and stratum moleculare and were characterized by arborized slender

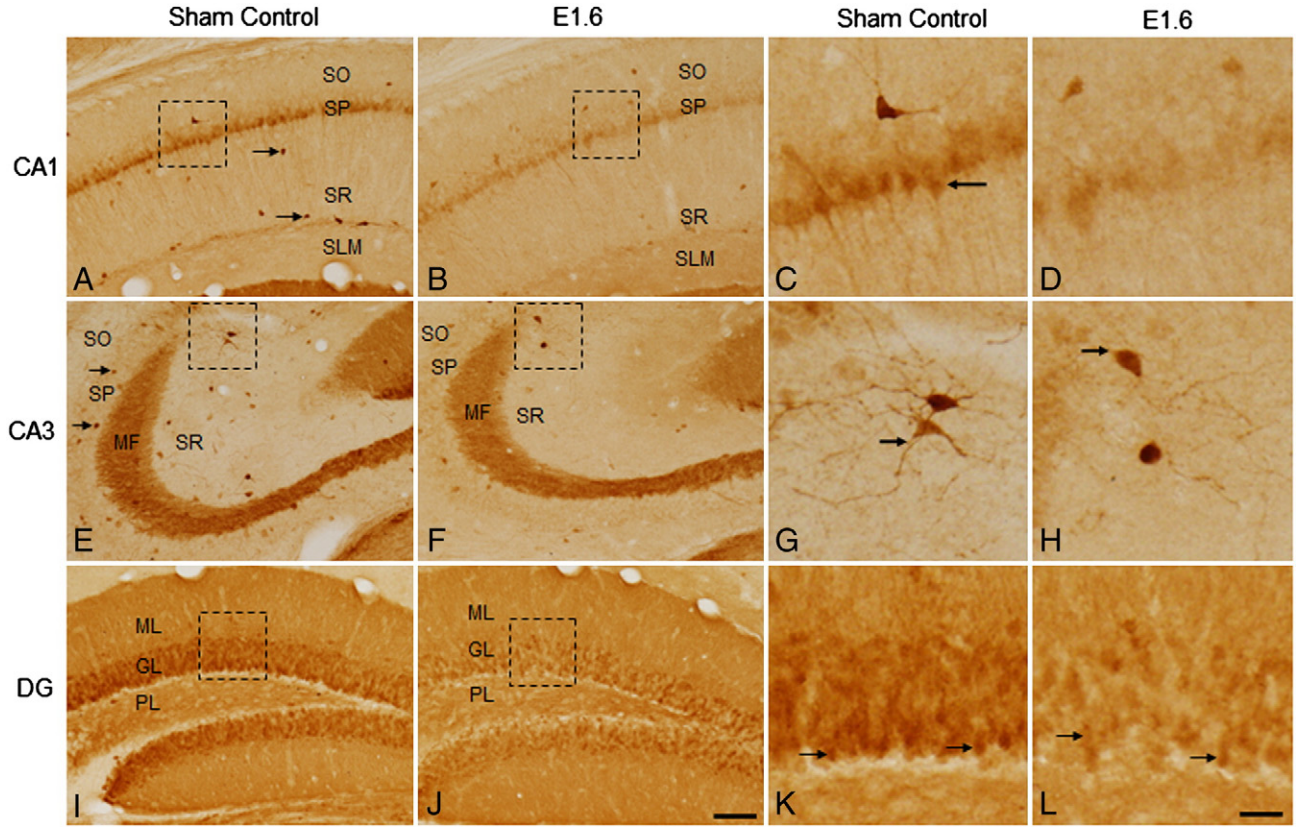

Fig. 1 – Distribution of calbindin D28-k (CB) immunoreactivity (IR) in the hippocampal CA1 area (A–D), CA3 area (E–H), and dentate gyrus (I–L) among sham control (SC) (SAR 0 W/kg) and exposed E1.6 (SAR 1.6 W/kg) groups after 3 months of radiofrequency exposure at 835 MHz. CB IR was observed in the pyramidal cells (A and C) of SP and interneurons (A) in SR (arrows) in SC group in the CA1 areas. Note the loss of interneurons (B) and decrease of the pyramidal cells in SP in E1.6 group (B and D). CB immunoreactive neurons (arrows) in the SR of CA3 area displayed morphological changes with loss of dendritic arborization in the E1.6 group (E–H). Decrease of pyramidal cells (arrows) as well as loss CB IR of mossy fibers was noted in the E1.6 group (H). Decrease in the density of CB IR was observed in all the three layers of the dentate gyrus of the E1.6 group as compared with the SC group (I and J). Note disruption of the alignment and loss of the granule cells (arrows) in granular layer of the E1.6 group (K and L). SO, stratum oriens; SP, stratum pyramidale; SR, stratum radiatum; SLM, stratum lacunosum moleculare; MF, mossy fibers; ML, molecular layer; GL, granular layer; PL, polymorphous layer. Scale bars: 100 μm (A, B, E, F, I, and J), 50 μm (C, D, G, H, K, and L).

processes (Figs. 1A and C). Compared with SC group, only a few pyramidal cells showed CB IR in the stratum pyramidale of the exposed (E1.6) group indicating loss of pyramidal cells (Figs. 1B and D). Few interneurons were faintly stained and showed lack of arborization as well in the CA1 area of E1.6 group (Fig. 1B). Numerous immunoreactive fibers were prominently observed as running perpendicularly in the stratum radiatum of CA1 area in SC group while, in the E1.6 groups, those were very faint and incomplete (Figs. 1A–D). Stratum pyramidal as well as stratum radiatum in CA3 area of SC group displayed numerous CB immunoreactive multipolar and horizontally oriented cells with smooth dendritic processes (Figs. 1E–H). In the CA3 area of E1.6 group, CB IRs were weakly observed in the cell body of stratum pyramidale and stratum radiatum (Fig. 1F). In a few CB immunoreactive neurons, dendritic arborization also seemed to be absent in the E1.6 group (Fig. 1H). The mossy fiber also displayed weak CB IR in E1.6 group as compared with SC group (Figs. 1E and F).

In the SC group, the CB immunoreactive interneurons in the dentate gyrus were observed to be aligned at the junction between granular layer and polymorphous layer and was scattered abundantly in the granular layer (Figs. 1I and J). Along with a few CB immunoreactive interneurons, which showed weak IR, the alignment at the junction between granular layer and polymorphous layer was interrupted in the E1.6 group as well (Fig. 1L). The molecular layer in the SC group displayed CB immunoreactive cells along with fine vertically ascending fibers presumably the axons of the granule cells, while mossy fibers also appeared to be highly stained in the polymorphous layer. Such ascending fibers in the molecular layer as well as the mossy fibers were very faintly stained in the E1.6 group (Figs. 1I and J).

2.1.2. *GFAP Immunoreactivity*

The GFAP immunoreactive astrocytes were widely distributed through the CA1, CA3 area and the dentate gyrus in SC group.

In the stratum pyramidale of CA1 area, GFAP IR was absent in both SC and E1.6 groups (Figs. 2A and B). Except the stratum pyramidale, the GFAP immunoreactive astrocytes with elongated cytoplasmic processes were homogenously distributed in CA1 area of SC group. The GFAP immunoreactive astrocytes of CA1 areas in E1.6 group were shown to be hypertropic, heavily branched with prominently stained long cytoplasmic processes (Figs. 2C and D). Similar with CA1 area, the GFAP IR in CA3 area of E1.6 group was shown to be hypertrophic and/or hyperplastic with thickened and elongated processes (Figs. 2G and H). Such morphological alterations in the astrocytes indicate transformation into reactive astrocytes.

A relatively dense distribution of GFAP immunoreactive cells was observed in the dentate gyrus of both SC and E1.6 groups. In the molecular layer of the SC group, astrocytes were characterized by smaller stellate-shaped cell bodies and short processes while the astrocytes of E1.6 group appeared to be dense, highly stained with thicker and slightly elongated processes (Figs. 2A and B). Thick and darkly stained processes of GFAP immunoreactive cells appeared to be running through the granular layer of both groups (Figs. 2K and L). The number and the staining intensity of such processes were observed to be higher in the granular layer of E1.6 group. The GFAP immunoreactive astrocytes in the polymorphic layer of SC group had small cell bodies with short processes, while the GFAP IR of perikarya as well as its process appeared to be more prominent in E1.6 group.

2.2. *Immunoreactivity analysis*

2.2.1. *Calbindin immunoreactivity*

In the assessment of image analysis, the relative mean density of different subfields of the hippocampal regions was performed in SC and E1.6 groups to compare the CB IR distribution. CB IR was observed to be significantly lower in all the areas of the hippocampal formation in E1.6 group than those of the SC group (Fig. 3A). Both the groups displayed highest CB IR in the granular layer of the dentate gyrus and lowest was observed in the CA1 area. Significant difference was observed in the CA1 area ($p<0.01$), CA3 area ($p<0.05$),

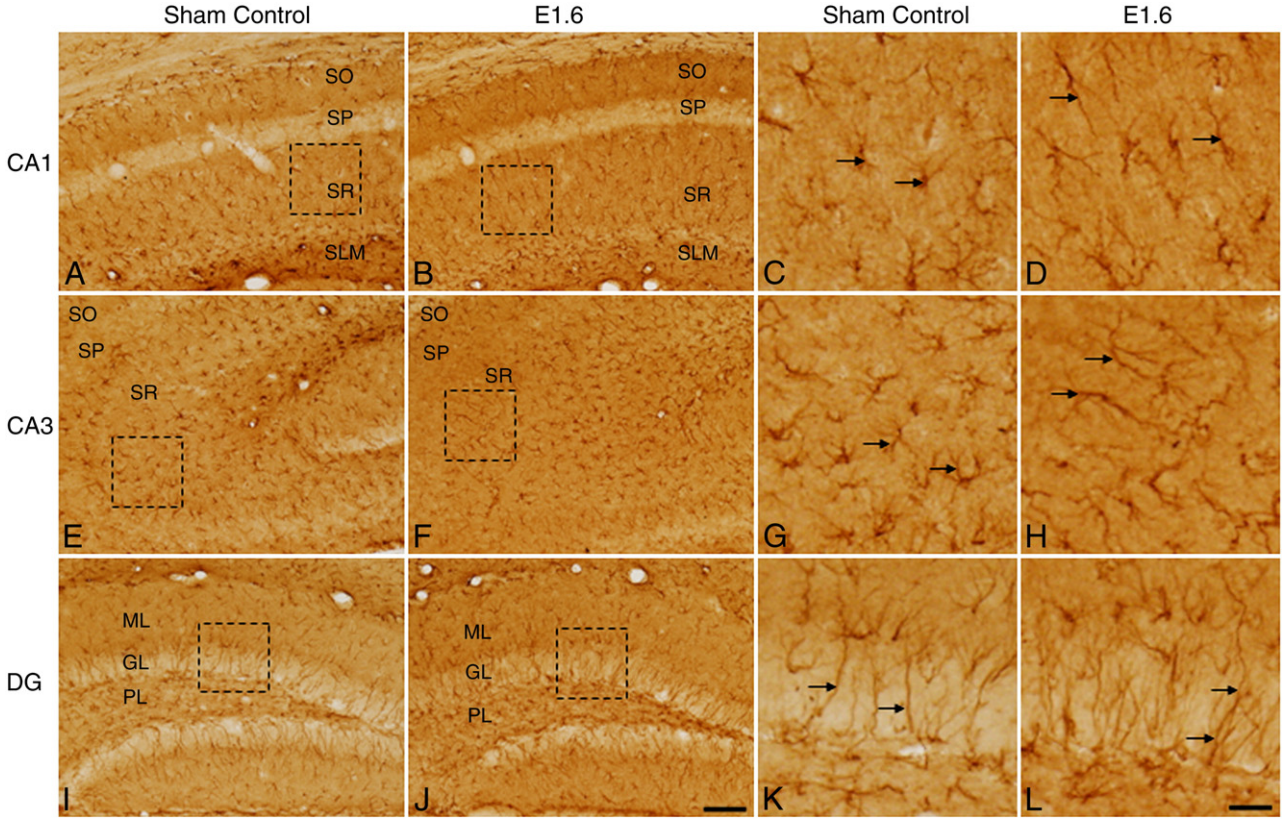

Fig. 2 – Distribution of GFAP immunoreactivity (IR) in the hippocampal CA1 area (A–D), CA3 area (E–H), and dentate gyrus (I–L) among sham control (SC) (SAR 0 W/kg) and exposed E1.6 (SAR 1.6 W/kg) groups after 3 months of radiofrequency exposure at 835 MHz. Astrocytes displaying GFAP IR was observed in all the layers of CA1 areas except SP (A–D). Note hypertrophic astrocytes (arrows) with heavily branched and elongated cytoplasmic processes in the E1.6 group as compared with the SC group (C and D). The cytoplasmic processes of the astrocytes (arrows) in the CA3 area were thickened and elongated in the E1.6 group as compared with the SC group (E–H). Alteration of the astrocytes signifies the transformation into reactive astrocytes. GFAP IR cells with thick and darkly stained process (arrows) appear to be running through the granular layer in both the groups (I–L). Astrocytes in the molecular and polymorphic layers of the E1.6 group appear to display higher GFAP IR as compared with SC group (I and J). SO, stratum oriens; SP, stratum pyramidale; SR, stratum radiatum; SLM, stratum lacunosum moleculare; ML, molecular layer; GL, granular layer; PL, polymorphous layer. Scale bars: 100 μm (A, B, E, F, I, and J), 50 μm (C, D, G, H, K, and L).

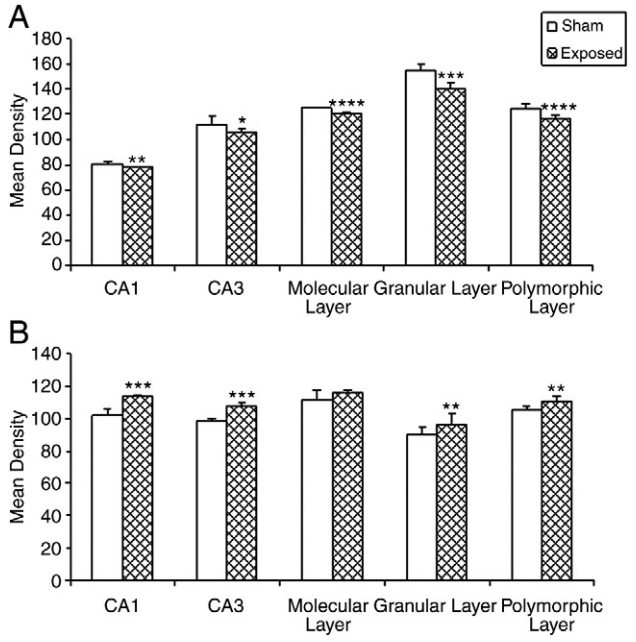

Fig. 3 – Observed changes in calbindin D28-k (A) and GFAP (B) IR presented by image analysis after radiofrequency exposure on the mean density in the hippocampal subfields (CA1, CA3, and dentate gyrus) of mice. (i) SC (sham control, SAR=0 W/kg) and (ii) E1.6 (exposed to low energy, SAR=1.6 W/kg). CA, cornu ammonis; ML, molecular layer; GL, granular layer; PL, polymorphous layer. $^{*}p<0.05$, $^{**}p<0.01$, $^{***}p<0.001$, $^{***}p<0.0001$.

molecular layer ($p<0.0001$), granular layer ($p<0.001$), and polymorphic layer ($p<0.0001$) of E1.6 group when compared with SC group (Fig. 3A).

2.2.2. *GFAP Immunoreactivity*

Relative mean density analysis was performed in SC and E1.6 groups to measure the GFAP IR in the areas of the hippocampal formation. GFAP IR was prominently observed in all the areas of the hippocampal formation except molecular layer in E1.6 groups as compared with SC group. In both groups, the most prominent GFAP IR was observed in the molecular layer and the lowest in the granular layer (Fig. 3B). Compared to the SC group, E1.6 group displayed significant difference in CA1 area ($p<0.001$), CA3 area ($p<0.001$), granular layer ($p<0.01$), and polymorphic layer ($p<0.01$). No significant difference was observed in the molecular layer of the dentate gyrus (Fig. 3B).

2.3. *Apoptosis*

To evaluate the apoptosis in the hippocampus, terminal deoxynucleotidyl transferase-mediated biotinylated UTP nick end labeling (TUNEL) staining was performed by using Trevigen Apoptotic Cell System (TACS) 2TdT-Fluor In Situ Apoptosis Detection Kit (4812-30-K). TUNEL-positive cells were observed in the CA1 and CA3 area of the E1.6 group. Majority of the TUNEL-positive cells in the CA1 area of E1.6 group was observed in the stratum pyramidale of CA1 area, while stratum oriens and stratum radiatum revealed few TUNEL-positive cells (Fig. 4E). TUNEL-positive cells were also noted in the CA3 area of E1.6 group, mainly in the stratum pyramidale (Fig. 4H). The E1.6 group exhibited numerous TUNEL-positive cells in the granular layer of the dentate gyrus with few isolated positive cells in the hilus (Fig. 4Q). In SC group, no TUNEL-positive cells were observed in all the three regions of the hippocampal region (Figs. 4B, H, and N). The PI-positive cells were observed in both the control and E1.6 groups in CA1, CA3, and dentate gyrus. PI-positive cells were mostly observed in the stratum pyramidale of CA1 (Figs. 4A and D) and CA3 (Figs. 4G and J) areas, while in the dentate gyrus, the granular layer exhibited majority of PI-positive cells (Figs. 4M and P). TUNEL assay revealed maximum percentage of TUNEL-positive cells in the granular layer of dentate gyrus followed by CA1 and CA3 areas, respectively (Table 1).

3. Discussion

The effect of RF exposure to the brain have been studied in the neuronal function, neuronal survival, learning and memory disturbances, and neurotransmitter release (Manikonda et al., 2007). By susceptibility to RF exposure, neuronal damages in the hippocampus, cortex as well as the basal ganglia in 12-26 weeks old rat has been reported (Salford et al., 2003). The hippocampus, especially the granule cells of the dentate gyrus (Odaci et al., 2008) and the CA areas (Bas et al., 2009a,b), is selectively vulnerable to RF exposure. Loss of pyramidal cells in the CA areas has been reported after prenatal period and 4 weeks of exposure at 900 MHz in adult rats (Bas et al., 2009a,b). EMF exposure has also resulted in the decrease of granule cell number in the rat dentate gyrus (Odaci et al., 2008). Similar studies of radiation effect have reported vulnerability of the granule cells in the dentate gyrus (Nagai et al., 2000; Jenrow et al., 2004). These previous reports may indicate the deleterious effect of RF exposure to the hippocampal formation.

Concurrent with the previous results, our study also showed loss of pyramidal cells in the CA areas as well as disruption in the granular layer of the dentate gyrus. The three subfields of the hippocampus (CA1 area, CA3 area, and dentate gyrus) constitute hippocampal trisynaptic circuit implicated with memory and learning (Tyler and DiScenna, 1984). Such selective losses of pyramidal cells in CA areas, granule cell in the dentate gyrus, and interneurons may give rise to learning and memory dysfunction. The loss of interneurons in the CA1 area, as shown in the present study, seems to be associated with complex cognitive, mnemonic, and emotional processes through its connection to the prefrontal regions (Barbas and Blatt, 1995).

CB, buffer type CaBP, is involved in regulating the intracellular Ca^{2+} concentration (Baimbridge et al., 1992) and has been proposed a protective role through its Ca^{2+}-buffering mechanism (Mattson et al., 1991). By this means, cytosolic CB in neuron might exert protective role against overfull calcium influx causing degenerative process. Interference on the intracellular Ca^{2+} homeostasis in the ion transport may alter ionic balance and lead to cell death (Liu and Fechter, 1996). Decrease in CB IR could be attributed to increased Ca^{2+} influx due to increased glutamate release or reduced postsynaptic

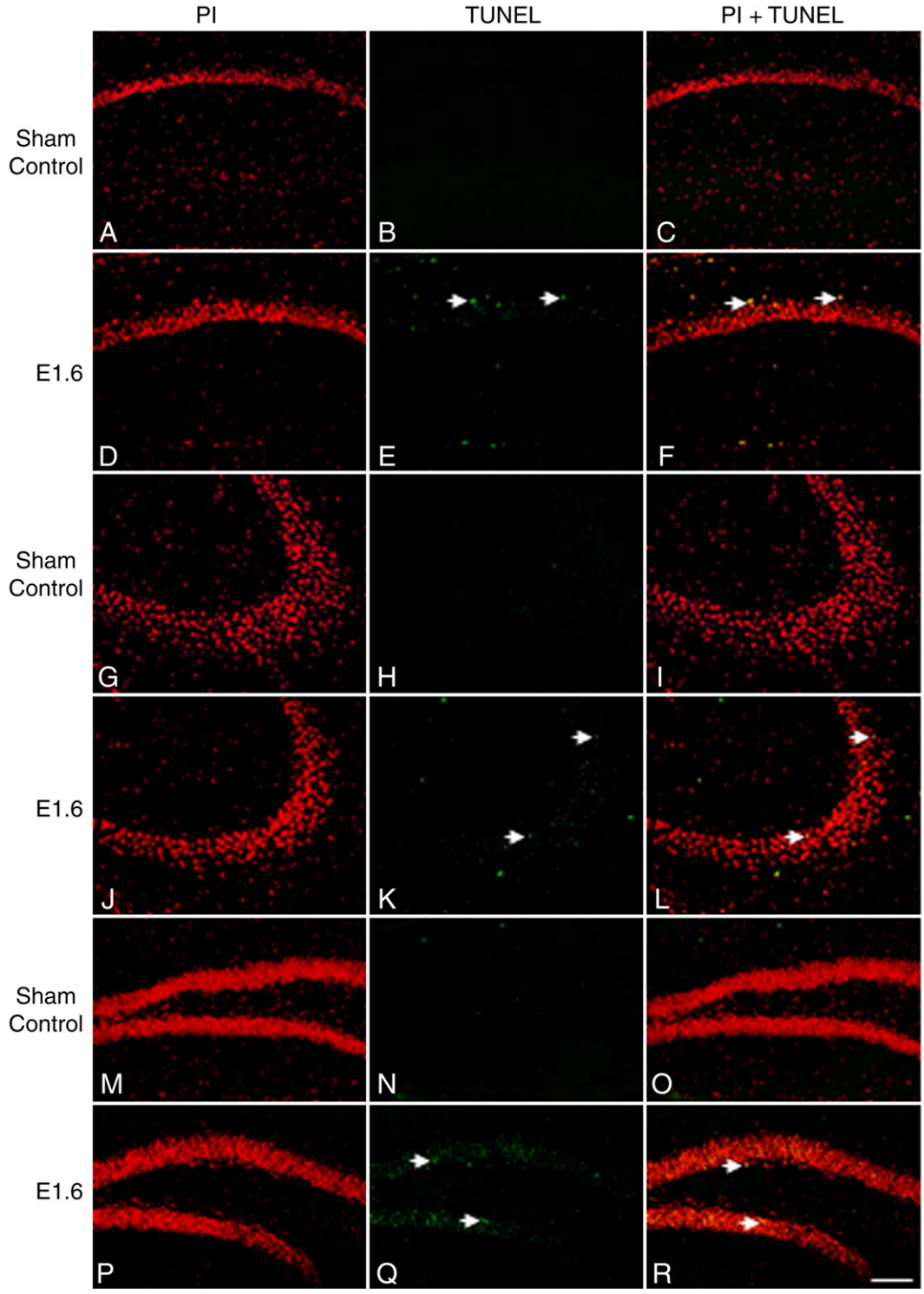

Fig. 4 – Representative photomicrographs showing propidium iodide (PI) and TUNEL labeling in the hippocampal subfields, CA1 area (A–F), CA3 area (G–L), and dentate gyrus (M–R) among sham control (SC) (SAR 0 W/kg) and exposed (E1.6) (SAR 1.6 W/kg) groups after 3 months of radiofrequency exposure at 835 MHz. PI counterstaining (red), TUNEL (green), and PI and TUNEL double staining (yellow). The stratum pyramidale in the CA1 (E), CA3 (K), and the granular layer of the dentate gyrus (Q) in the E1.6 group exhibited numerous TUNEL-positive cells (arrows). PI/TUNEL-positive cells (F, L, and R) can be visualized as yellow (arrows). Scale bar: 100 μm.

inhibition especially since transcription of CB gene has been reported to be inhibited by Ca^{2+} (Arnold and Heintz, 1997). Downregulation of CB expression has been associated with neuronal loss (Gonzalez et al., 2005). Compared with SC group, the prominent decrease of CB IR in all subfields of the hippocampal formation was observed in the E1.6 group

Table 1 – Summary of the expression of TUNEL-positive cell percentage in the hippocampal subfields (CA1 and CA3 areas and dentate gyrus) of sham control group (SC) and group exposed at 1.6 W/kg (E1.6) after 3 months of radiofrequency exposure at 835 MHz with low energy (specific absorption rate: SAR=1.6 W/kg). TUNEL-positive scores were evaluated as a percentage of "apoptotic" in PI-positive cells. PI staining was used as counter staining. (–), absence of TUNEL-positive cells; (+), 1–20%; (++), 21–40%. SC, sham control group; E1.6, exposed at SAR 1.6 W/kg group; CA, cornu ammonis; DG, dentate gyrus.

	SC group (n=5)	E1.6 group (n=5)
CA1 area	–	++
CA3 area	–	+
DG	–	++

(Fig. 3A). Hence, in E1.6 groups, the decrease of CB IR and loss of CB immunoreactive neurons in the hippocampus ascribed in the RF exposure imply the decrease of Ca^{2+}-buffering capability and may lead to cell death. Disruption of the granule cell alignment at the junction of granular and polymorphous layer associated with loss of the granule cells further strengthens the reason for loss of CB IR due to increased Ca^{2+} influx.

Reactive astrocytosis linked with Ca^{2+} influx (Lee et al., 2000) occurs after various CNS injuries (Eng et al., 1992) and is an early response of astrocytes to injury (Little and O'Callaghan, 2001). Reactive astrocytosis by EMF exposure could be elicited by deleterious stimuli like thermal effect (Miller et al., 1987), oxidative stress, which might be produced in the EMF exposed brain (Morgan et al., 1997; Meral et al., 2007). Compared with the SC group, the increase of GFAP IR in the hippocampal formation (CA1, CA3, molecular layer, granular layer, and polymorphous layer) of the E1.6 group was also observed (Fig. 3B). The increase of GFAP IR in the present study was well correlated with morphological and functional changes of reactive astrocytosis, which commonly precedes neuronal death (Petito and Halaby, 1993). In line with our data, reactive astrocytosis was also observed in rats after chronic exposure of 900 MHz at SAR 6 W/kg (Ammari et al., 2008). Neuron and glial cell interaction, where glial cells control Ca^{2+} signal to facilitate itself to incorporate extracellular signals (Verkhratsky and Kettenmann, 1996), is essential for Ca^{2+}-mediated neuronal activity and regulation of synaptic transmission. The imbalance of Ca^{2+} homeostasis following alterations in signal transduction through RF exposure may cause insult to elicit apoptosis in the brain.

EMF exposure has been known to induce apoptosis in human colon cancer cells (Maeda et al., 2004) and human epidermoid cancer cells (Caraglia et al., 2005), while on the contrary, no apoptosis was observed in human peripheral blood mononuclear cells (Capri et al., 2004a) as well as human lymphocytes (Capri et al., 2004b). In the present study, TUNEL-positive cells in the CA1, CA3, and the granular layer of the dentate gyrus were identified in the E1.6 group only (Figs. 4E, K, and Q). The TUNEL-positive cells in the pyramidal cell layer of the CA1 region of the E1.6 group (Fig. 4E) are well correlated with the loss of CB immunoreactive pyramidal cells (Figs. 1B and D). The disruption of the granule cells in the E1.6 group (Fig. 1L) is also well matched with the abundant TUNEL-positive cells in the granular layer of the dentate gyrus (Fig. 4Q). However, neuronal losses in the hippocampal subfields were not identified in 1 month of RF exposure, although decrease of CB IR in the hippocampus was observed (Maskey et al., 2010). This may indicate that chronic exposure to the RF may be more harmful to the hippocampus neuron concerning behavior, learning, and memory impairment, as compared to the short-duration RF exposure even at the same frequency.

Consequently, the occurrence of long-term RF exposure in the hippocampus resulted in the decrease of CB IR accompanying apoptosis and increase of GFAP IR, which might be used as morphological parameters in the RF exposure damages. Hence, for preventing possible harmful effects from long-term RF exposure in advance, elucidating and clarifying the molecular cascade of apoptosis signal in the hippocampus may be needed.

4. Experimental procedures

4.1. *Animals experimentation*

Male ICR mice (6 weeks old), 20–30 g (Orientbio Inc.) (n=20), were used for the experiment. The mice were kept under controlled conditions (ambient temperature of 20 to 25 °C, 12-h light/dark cycle). Food (Samtako Bio Korea, Osan, South Korea) and water were supplied *ad libitum*. NIH's guidelines for animal research were followed for all animal procedures and were approved by Dankook University's Institutional Animal Care and Use Committee (DUIAC), which adheres to the guidelines issued by the Institution of Laboratory of Animal Resources (ILAR).

4.2. *Exposure system*

The exposure system (Wave Exposer V20) has been described in detail elsewhere (Maskey et al., 2010). Briefly, a Wave Exposer V20 emitting 835 MHz equivalent to the Korean CDMA mobile phone frequency was designed by the Division of Information Technology Engineering, Soonchunhyang University, (Maskey et al., 2010). Specific absorption rate (SAR) was controlled from 1.6 to 4.0 W/kg, which is the same value as electric field intensity between 59.56 and 94.18 V/m for muscle (=0.92, =57, and =1020 kg/m^3) on 835-MHz CDMA frequency. Waves were generated and amplified in an electronic unit and, eventually, were radiated by a pyramidal rectangular horn antenna connected by a waveguide to coaxial transition. Standard mouse cage of 22 inches was used for the apparatus. Output powers of horn antenna of the exposure apparatus are 2.5 W for SAR 1.6 W/kg and 6.3 W for SAR 4.0 W/kg. Electric field intensities due to SAR values can be calculated, and power value was obtained by a computer simulation with HFSS (High Frequency Structure Simulator) manufactured by Ansoft Co. (Pittsburgh, PA). Five cylinder-shaped models of mice were used for simulation. The simulation variable was both the mice location and the distance from the horn aperture for freely moving mice. Power was obtained by averaging the simulated peak electric field intensities on each mouse body. The wave exposure from horn antenna to the

mouse cage was provided by wave absorption material (TDK ceramic absorber) mimicking the radiation exposure in the open environment, which limits the influence the number of mice might have on exposure. The exposure apparatus provides an automatic light system and air conditioning system with a water feeder, with no restriction in movement during exposure eliminating stress during exposure.

4.3. *Experimental design*

Mice were exposed to 835 MHz of radiation with an average SAR of 1.6 W/kg using Wave Exposer V20. The mice were divided randomly into 2 groups ($n=10$): (1) a sham control group (SC) (SAR=0 W/kg) and (2) a group exposed to low energy (E1.6) (SAR=1.6 W/kg). All groups were exposed 8 h/d for 3 months. Three hours after the final exposure, animals were anesthetized with diethyl ether, and their brains were collected using perfusion and fixation with phosphate-buffered saline (PBS) and 4% paraformaldehyde (PFA) solution. Anesthesia was also used to avoid animal stress and to lower the augmentation of blood pressure during perfusion and fixation.

4.4. *Immunohistochemical analysis*

After decapitation, the brains were immediately removed, postfixed overnight in 4% PFA, and cryoprotected by infiltration with a sucrose series (10%, 20%, and 30%) solution at 4 °C. Forty-micrometer coronal sections were obtained on a freezing sliding microtome and collected in six-well plates. Five slides of each cortical area were selected from each mouse and measured all specifically stained cells in corresponding areas. Brain areas were identified based on the atlas of the mouse brain by Paxinos and Franklin (2001). Immunohistochemistry was performed with the free-floating method, as described earlier (Maskey et al., 2010). Briefly, coronal sections of the hippocampal region were incubated for 48 h at 4 °C with primary antibodies, polyclonal anti-rabbit calbindin D28-k (1:4000; AB1778; Millipore, CA, USA) and polyclonal anti-rabbit GFAP (1:15,000; AB7260; Abcam, Cambridge, UK) in blocking buffer containing 1% bovine serum albumin, 0.3% Triton X-100, and 1% normal horse serum. To eliminate peroxidase activity, the sections were treated with 10% hydrogen peroxide in PBS. The sections were washed thrice for 10 min in PBS. Incubation with biotinylated secondary antibodies at 1:250 for 1.5 h at room temperature was followed by treatment with an avidin–biotin–peroxidase complex (Vectastain ABC Mouse Elite Kit; Vector Laboratories, Burlingame, CA, USA). After three washes in PBS, the sections were stained in a distilled water solution containing diaminobenzidine (DAB) and hydrogen peroxide for 5 min. Sections from each group were stained together to minimize variability. Following additional washes, sections were mounted on gelatin-coated slides, dehydrated in ethanol, cleared in xylene, and cover slipped with DPX.

4.5. *Apoptosis*

For terminal deoxynucleotidyl transferase-mediated biotinylated UTP nick end labeling (TUNEL) analysis, the brains of the mice from both groups (SC and E1.6) were obtained after perfusing with 0.1 M phosphate buffer and 4% PFA respectively. The brains were fixed overnight in 4% PFA followed by series of sucrose (10%, 20%, and 30%) solutions at 4 °C. Sections of 20 μm were obtained, and TUNEL staining was performed using the Trevigen Apoptotic Cell System (TACS) 2TdT-Fluor In Situ Apoptosis Detection Kit (4812-30-K) according to the manufacturer's instruction.

Briefly, the slides were incubated with proteinase K (4800-30-01) for 1 h at room temperature, which was followed by immersion in TdT labeling buffer (4810-30-02) for 5 min. Sections were then incubated in 50 μl of Labeling Reaction Mix (1 μl TdT dNTP Mix (4810-30-04), 1 μl TdT Enzyme (4810-30-05), 50× Cation Stock, 50 μl of 1× TdT Labeling Buffer for each slides) for terminal deoxynucleotidyl transferase enzyme linkage of dUTP-digoxigenin to the 3′-OH DNA ends at 37 °C for 1 h in humidity chamber. The reaction was terminated by incubation with 1× TdT stop buffer (4810-30-03) for 5 min at room temperature. Following washing with double-distilled water, the slides were treated with Strep-Fluor solution for 20 min in dark. After washing with PBS (3×10 min) propidium iodidie (PI) was used for counter staining for 30 min in dark. Mounting was performed with fluorescence mounting medium (Biomeda Corp, CA, USA). For the TUNEL reaction, the PI-stained cells served as controls. Five slides from each group were used for the purpose of TUNEL-positive cell count. The semiquantitative TUNEL-positive score were evaluated as a percentage of "apoptotic" and PI-positive cells as follows: (–), absence of TUNEL-positive cells; (+), 1–20%; (++), 21–40%; strong TUNEL-positive was defined at more than 40%.

4.6. *Image analysis*

Analysis was performed with an Olympus BX 51 microscope in the CA1, CA3, and dentate gyrus (molecular, granular, and polymorphous layer), and pictures were taken by a digital camera system (DP50, Olympus, Japan). The NIH image program (Scion Image) was used to determine staining densities as described previously (Maskey et al., 2010). The investigator performing the analysis was blinded to the groups' identification.

4.7. *Statistical analysis*

Data are expressed as mean±SD. Comparison of the mean density of the different subfields of the hippocampus (CA1, CA3, and dentate gyrus) between the sham control group and exposed group (E1.6) was done by unpaired Student's *t*-test. Differences were considered significant at $p<0.05$.

Acknowledgments

The present research was conducted by a research fund from the Institute of Bio-science and Technology at Dankook University in 2009.

REFERENCES

Adey, W.R., 1981. Tissue interactions with non-ionising electromagnetic fields. Physiol. Rev. 61, 435–514.

Adey, W.R., Bawin, S.M., Lawrence, A.F., 1982. Effects of weak amplitude-modulated microwave fields on calcium efflux

from awake cat cerebral cortex. Bioelectromagnetics 3, 295–307.
Airaksinen, M.S., Eilers, J., Garaschuk, O., Thoenen, H., Konnerth, A., Meyer, M., 1997. Ataxia and altered dendritic calciums signaling in mice carrying a targeted null mutations of calbindin D28k gene. Proc. Natl Acad. Sci. USA 94, 1488–1493.
Ammari, M., Brillaud, E., Gamez, C., Lecomte, A., Sakly, M., Abdelmelek, H., de Seze, R., 2008. Effect of a chronic GSM 900 MHz exposure on glia in the rat brain. Biomed. Pharmacother. 62, 273–281.
Araque, A., Carmignoto, G., Haydon, P.G., 2001. Dynamic signaling between astrocytes and neurons. Annu. Rev. Physiol. 63, 795–813.
Arnold, D.B., Heintz, N., 1997. A calcium responsive element that regulates expression of two calcium binding proteins in Purkinje cells. Proc. Natl Acad. Sci. USA 94, 8842–8847.
Artola, A., Singer, W., 1993. Long-term depression of excitatory synaptic transmission and its relationship to long-term potentiation. Trends Neurosci. 16, 480–487.
Baimbridge, K.G., Celio, M.R., Rogers, J.H., 1992. Calciumbinding proteins in the nervous system. Trends Neurosci. 15 (8), 303–308.
Barbas, H., Blatt, G.J., 1995. Topographically specific hippocampal projections target functionally distinct prefrontal areas in the rhesus monkey. Hippocampus 5, 511–533.
Bas, O., Odaci, E., Mollaoglu, H., Ucok, K., Kaplan, S., 2009a. a. Chronic prenatal exposure to the 900 megahertz electromagnetic field induces pyramidal cell loss in the hippocampus of newborn rats. Toxicol. Ind. Health 25, 377–384.
Bas, O., Odaci, E., Kaplan, S., Acer, N., 2009b. b. 900 MHz electromagnetic field exposure affects qualitative and quantitative features of hippocampal pyramidal cells in adult rat. Brain Res. 1265, 178–185.
Bawin, S.M., Adey, W.R., Sabbot, I.M., 1978. Ionic factors in release of 45Ca2þ from chicken cerebral tissue by electromagnetic fields. Proc. Natl Acad. Sci. USA 75, 6314–6318.
Behari, J., Kunjilwar, K.K., Pyne, S., 1998. Interaction of low level modulated RF radiation with Na^+–K^+-ATPase. Bioelectrochem. Bioenerg. 47, 247–252.
Blackman, C.F., 1992. Calcium release from neural tissue: experimental results and possible mechanisms. In: Norden, B., Ramel, C. (Eds.), Interaction Mechanisms of Low-Level Electromagnetic Fields in Living Systems. Oxford University Press, Oxford, pp. 107–129.
Borbely, A.A., Huber, R., Graf, T., Fuchs, B., Gallmann, E., Achermann, P., 1999. Pulsed high-frequency electromagnetic field affects human sleep and sleep electroencephalogram. Neurosci. Lett. 275, 207–210.
Brillaud, E., de Seze, R., 2006. Telephones mobiles et neurotoxicite pour le systeme nerveuz central. Environnement Risques et Sante 5.
Capri, M., Scarcella, E., Bianchi, E., Fumelli, C., Mesirca, P., Agostini, C., Remondini, D., Schuderer, J., Kuster, N., Franceschi, C., Bersani, F., 2004a. 1800 MHz radiofrequency (mobile phones, different global system for mobile communication modulations) does not affect apoptosis and heat shock protein 70 level in peripheral blood mononuclear cells from young and old donors. Int. J. Radiat. Biol. 80, 389–397.
Capri, M., Scarcella, E., Fumelli, C., Bianchi, E., Salvioli, S., Mesirca, P., Agostini, C., Antolini, A., Schiavoni, A., Castellani, G., Bersani, F., Franceschi, C., 2004b. *In vitro* exposure of human lymphocytes to 900 MHz CW and GSM modulated radiofrequency: studies of proliferation, apoptosis and mitochondrial membrane potential. Radiat. Res. 162, 211–218.
Caraglia, M., Marra, M., Mancinelli, F., D'Ambrosio, G., Massa, R., Giordano, A., Budillon, A., Abbruzzese, A., Bismuto, E., 2005. Electromagnetic fields at mobile phone frequency induce apoptosis and inactivation of the multi-chaperone complex in human epidermoid cancer cells. J. Cell. Physiol. 204, 539–548.
Celio, M., Pauls, T., Schwaller, B. (Eds.), 1996. Guidebook to the Calcium Binding Proteins. Oxford University Press, Oxford.
D'Andrea, J.A., Chou, C.K., Johnston, S.A., Adair, E.R., 2003. Microwave effects on the nervous system. Bioelectromagnetics l6, S107–S147.
Dutta, S.K., Subramoniam, A., Ghosh, B., Parshad, R., 1984. Microwave radiation-induced calcium ion efflux from human neuroblastoma cells in culture. Bioelectromagnetics 5, 71–78.
Dutta, S.K., Ghosh, B., Blackman, C.F., 1989. Radiofrequency radiation induced calcium ion efflux enhancement from human and other neuroblastoma cells in culture. Bioelectromagnetics 10, 197–202.
Eddleston, M., Mucke, L., 1993. Molecular profile of reactive astrocytese implications for their role in neurologic disease. Neuroscience 54, 15–36.
Edelstyn, N., Oldershaw, A., 2002. The acute effects of exposure to the electromagnetic field emitted by mobile phones on human attention. NeuroReport 13, 119–121.
Eng, L.F., 1985. Glial fibrillary acidic protein (GFAP): the major protein of glial intermediate filaments in differentiated astrocytes. J. Neuroimmunol. 8, 203–214.
Eng, L.F., Shiurba, R.A., 1988. Glial fibrillary protein acidic protein: a review of structure function and clinical application. In: Marangos, P.J., Campbell, I., Cohen, R.M. (Eds.), Neuronal and Glial Proteins: Structure, Function and Clinical Application, vol. 2. Academic Press, New York, pp. 339–359.
Eng, L.F., Yu, A.C.H., Lee, Y.L., 1992. Astrocytic response to injury. Prog. Brain Res. 94, 353–365.
Eng, L.F., Ghirnikar, R.S., Lee, Y.L., 2000. Glial fibrillary acidic protein: GFAP-thirty-one years (1969–2000). Neurochem. Res. 25, 1439–1451.
Feychting, M., Ahlbom, A., Kheifets, L., 2005. EMF and health. Annu. Rev. Public Health 26, 165–189.
Frey, A.H., 1998. Headaches from cellular telephones: are they real and what are the implications. Environ. Health Perspect. 106, 101–103.
Gonzalez, D., Satriotomo, I., Miki, T., Lee, K.Y., Yokoyama, T., Touge, T., Matsumoto, Y., Li, H.P., Kuriyama, S., Takeuchi, Y., 2005. Effects of monocular enucleation on calbindin-D 28k and c-Fos expression in the lateral geniculate nucleus in rats. Okajimas Folia Anat. Jpn 82, 9–18.
Hamblin, D.L., Wood, A.W., 2002. Effects of mobile phone emissions on human brain activity and sleep variables. Int. J. Radiat. Biol. 78, 659–669.
Hietanen, M., 2006. Establishing the health risks of exposure to radiofrequency fields requires multidisciplinary research. Scand. J. Work. Environ. Health. 32,169–170.
Hocking, B., 1998. Preliminary report: symptoms associated with mobile phone use. Occup. Med. 48, 357–360.
Hossmann, K.A., Hermann, D.M., 2003. Effects of electromagnetic radiation of mobile phones on the central nervous system. Bioelectromagnetics 24, 49–62.
International Commission for Non-Ionizing Radiation Protection, 2004. Epidemiology of health effects of radiofrequency exposure. Environ. Health Perspect. 112, 1741–1754.
Jenrow, K.A., Ratkewicz, A.E., Lemke, N.W., Kadiyala, M., Zalinski, D.N., Burdette, D.E., Elisevich, K.V., 2004. Effects of kindling and irradiation on neuronal density in the rat dentate gyrus. Neurosci. Lett. 371, 45–50.
Koivisto, M., Krause, C.M., Revonsuo, A., Laine, M., Hämäläinen, H., 2000a. The effects of electromagnetic field emitted by GSM phones on working memory. NeuroReport 11, 1641–1643.
Koivisto, M., Revonsuo, A., Krause, C., Haarala, C., Sillanmäki, L., Laine, M., Hämäläinen, H., 2000b. Effects of 902 MHz electromagnetic field emitted by cellular telephones on response times in humans. NeuroReport 11, 413–415.
Kunjilwar, K.K., Behari, J., 1993. Effect of amplitude modulated radiofrequency radiation on cholenergic system of developing rats. Brain Res. 601, 321–324.

Lee, Y.B., Du, S., Rhim, H., Lee, E.B., Markelonis, G.J., Oh, T.H., 2000. Rapid increase in immunoreactivity to GFAP in astrocytes *in vitro* induced by acidic pH is mediated by calcium influx and calpain I. Brain Res. 864, 220–229.

Liang, C.L., Sinton, C.M., Sonsalla, P.K., German, D.C., 1996. Midbrain dopaminergic neurons in the mouse that contain calbindin-D28k exhibit reduced vulnerability to MPTP-induced neurodegeneration. Neurodegeneration 5, 313–318.

Lisman, J., 1989. A mechanism for the Hebb and the anti-Hebb processes underlying learning and memory. Proc. Natl Acad. Sci. USA 86, 9574–9578.

Little, A.R., O'Callaghan, J.P., 2001. Astrogliosis in the adult and developing CNS: is there a role for proinflammatory cytokines? Neurotoxicology 22, 607–618.

Liu, Y., Fechter, L.D., 1996. Comparison of the effects of trimethyltin on the intracellular calcium levels in spiral ganglion cells and outer hair cells. Acta Otolaryngol. 116, 417–421.

Maeda, K., Maeda, T., Qi, Y., 2004. *In vitro* and *in vivo* induction of human LoVo cells into apoptotic process by non-invasive microwave treatment: a potentially novel approach for physical therapy of human colorectal cancer. Oncol. Rep. 11, 771–775.

Manikonda, P.K., Rajendra, P., Devendranath, D., Gunasekaran, B., Channakeshava, Aradhya, R.S., Sashidhar, R.B., Subramanyam, C., 2007. Influence of extremely low frequency magnetic fields on Ca^{2+} signaling and NMDA receptor functions in rat hippocampus. Neurosci. Lett. 413, 145–149.

Maskey, D., Kim, M., Aryal, B., Pradhan, J., Choi, I.Y., Park, K.S., Son, T., Hong, S.Y., Kim, S.B., Kim, H.G., Kim, M.J., 2010. Effect of 835 MHz radiofrequency radiation exposure on calcium binding proteins in the hippocampus of the mouse brain. Brain Res. 1313, 232–241.

Mattson, M.P., Rychlik, B., Chu, C., Christakos, S., 1991. Evidence for calcium-reducing and excitoprotective roles for the calcium-binding protein-D28k in cultured hippocampal neurons. Neuron 6, 41–51.

Mausset, A.L., de Seze, R., Montpeyroux, F., Privat, A., 2001. Effects of radiofrequency exposure on the GABAergic system in the rat cerebellum: clues from semiquantitative immunohistochemistry. Brain Res. 912, 33–46.

Meral, I., Mert, H., Mert, N., Deger, Y., Yoruk, I., Yetkin, A., Keskin, S., 2007. Effects of 900-MHz electromagnetic field emitted from cellular phone on brain oxidative stress and some vitamin levels of guinea pigs. Brain Res. 1169, 120–124.

Miguel-Hidalgo, J.J., Wei, J., Andrew, M., Overholser, J.C., Jurjus, G., Stockmeier, C.A., Rajkowska, G., 2002. Glia pathology in the prefrontal cortex in alcohol dependence with and without depressive symptoms. Biol. Psychiatry 52, 1121–1133.

Miller, R.J., 1995. Regulation of calcium homoeostasis in neurons: the role of calcium-binding proteins. Biochem. Soc. Trans. 23, 629–632.

Miller, D.B., Blackman, C.F., O'Callaghan, J.P., 1987. An increase in glial fibrillary acidic protein follows brain hyperthermia in rats. Brain Res. 415, 371–374.

Morgan, T.E., Rozovsky, I., Goldsmith, S.K., Stone, D.J., Yoshida, T., Finch, C.E., 1997. Increased transcription of the astrocyte gene GFAP during middle-age is attenuated by food restriction: implications for the role of oxidative stress. Free Radic. Biol. Med. 23, 524–528.

Nagai, R., Tsunoda, S., Hori, Y., Asada, H., 2000. Selective vulnerability to radiation in the hippocampal dentate granule cells. Surg. Neurol. 53, 503–506 discussion 506-507.

Norton, W.T., Aquino, D.A., Hozumi, I., Chiu, F.C., Brosnan, C.F., 1992. Quantitative aspects of reactivee gliosis: a review. Neurochem. Res. 17, 877–885.

Odaci, E., Bas, O., Kaplan, S., 2008. Effects of prenatal exposure to a 900 megahertz electromagnetic field on the dentate gyrus of rats: a stereological and histopathological study. Brain Res. 1238, 224–229.

Paxinos, G., Franklin, K.B.J., 2001. The Mouse Brain in Stereotaxic Coordinates, Second edition. Academic Press, San Diego.

Petito, C.K., Halaby, I.A., 1993. Relationship between ischemia and ischemic neuronal necrosis to astrocyte expression of glial fibrillary acidic protein. Znt. J. Deu. Neurosci. 11, 239–247.

Pfeiffer, B., Norman, A.W., Hamprecht, B., 1989. Immunocytochemical characterization of neuron-rich rat brain primary cultures: calbindin D28k as marker of neuronal subpopulation. Brain Res. 476, 120–128.

Preece, A.W., Iwi, G., Davies-Smith, A., Wesnes, K., Butler, S., Lim, E., Varey, A., 1999. Effect of a 915-MHz simulated mobile phone signal on cognitive function in man. Int. J. Radiat. Biol. 75, 447–456.

Salford, L.G., Brun, A.E., Eberhardt, J.L., Malmgren, L., Persson, B.R., 2003. Nerve cell damage in mammalian brain after exposure to microwaves from GSM mobile phones. Environ. Health Perspect. 111, 881–883.

Tyler, T.J., DiScenna, P., 1984. The topological anatomy of the hippocampus: a clue to its function. Brain Res. Bull. 6, 711–719.

Verkhratsky, A., Kettenmann, H., 1996. Calcium signaling in glial cells. Trends Neurosci. 9, 346–352.

Wagner, P., Roschke, J., Mann, K., Hiller, W., Frank, C., 1998. Human sleep under the influence of pulsed radiofrequency electromagnetic fields: a polysomnographic study using standardized conditions. Bioelectromagnetics 19, 199–202.